Measurement of Switching Transient Overvoltages with a Capacitive Electric Field Sensor

Felipe L. Probst, Michael Beltle, Malte Gerber, Stefan Tenbohlen, Kai A. Alsdorf

***Abstract*--This paper presents a case study of measurements of switching transient overvoltages using a capacitive electric field sensor. The system was developed and installed in a substation after the failure of a surge arrester during the energization of a 420 kV transmission line. First, the closing operation was simulated in an electromagnetic transient simulation program to estimate the switching transient overvoltages for this event. Then, the concept and design of the measurement system are explained. The system calibration performed in the high-voltage laboratory is presented. Afterward, the installation of the measurement system in the substation is discussed, with a special focus on the calibration of the voltage ratio considering the physical configuration where it is installed. Finally, the measurement results are presented and compared with simulations. The results show that the transient overvoltages caused by the energization of the transmission line should not cause the failure of the surge arrester. The measurement system has been demonstrated to be capable of measuring switching transient voltages of a 420 kV transmission line and can be considered a flexible solution for the long-term monitoring of transient overvoltages in substations.**

***Keywords*: Capacitive Electric Field Sensor, EMTP Simulation, High Voltage Power Quality Measurement, Measurement System Design, Switching Overvoltage, Transient Overvoltage Measurement.**

I. Introduction

THE equipment installed in a high-voltage substation must withstand fast current and voltage variations, known as electromagnetic transients, despite operating in a steady state most of the time [1] - [7]. These transients can occur due to external events, such as lightning discharges, or due to recurring events in power system operation, such as the energization of transformers and transmission lines [8].

In substations above 123 kV, Capacitive Voltage Transformers (CVTs) are generally used for voltage measurement at power frequency (e.g. 50 Hz). However, the output voltage of a CVT is distorted for high-frequency signals due to the constructive characteristics with inductive and capacitive components [9], [10]. To accurately measure fast transients such as lightning or switching, one solution is to correct the output voltage of the CVT, for which several methods have been applied [10] - [13]. Another approach, of course, is to use broadband devices to measure these transients correctly, such as voltage sensors connected to transformer bushings [14] - [16], and electric field sensors.

This paper presents a measurement system designed to measure transient overvoltages during the energization of a 420 kV transmission line using capacitive electric field sensors. During the energization of a transmission line, when the line was closed on one side (substation B) and open on the other side (substation A), a surge arrester in substation A failed. No digital disturbance recorder was installed, so the transient voltage during the failure is unknown. Therefore, an investigation was initiated to analyze whether the transient overvoltage could be high enough to cause the failure.

First, a time-domain simulation was performed by modeling the transmission line and substations in ATP (Alternative Transient Program) and evaluating the voltage during the line energization. Then, a measurement device has been designed and installed at an air-insulated disconnector in substation A. The device is based on the principle of a capacitive electric field sensor and works as a capacitive voltage divider, considering the stray capacitance C_1 between the switch and a coupling plane and the capacitance C_2 calculated according to the expected output voltage (see Section III). Three devices have been installed, one at each phase. The output voltages are continuously recorded with a broadband power quality monitoring system, and the recorded transients are available online. Finally, the measured values are compared to simulations.

II. Simulation of Electromagnetic Transients During the Switching Operation

The first objective of the case study was to evaluate whether the switching transient voltages during the energization of the transmission line between substations A and B (line A-B) could be high enough to cause a malfunction in the equipment connected to this line, especially in the surge arresters. Therefore, the investigation started with the simulation of the energization event in the electromagnetic transient simulation program ATP. Fig. 1 shows the schematic diagram of the circuit implemented in ATP.

The transmission line A-B has a nominal voltage of 420 kV and a length of 200 km. Therefore, it is considered a long line and was modeled with a distributed parameter model with concentrated losses based on the traveling wave method of Bergeron [17], with the parameters calculated at the fundamental frequency (50 Hz). This method is widely used to model transmission lines for transient studies and was chosen due to its low computational load.

F. L. Probst, M. Beltle, M. Gerber and S. Tenbohlen are with the Institute of Power Transmission and High Voltage Technology (IEH), University of Stuttgart, Stuttgart, 70569 Germany (email: felipe-luis.probst@ieh.uni-stuttgart.de; michael.beltle@ieh.uni-stuttgart.de; malte.gerber@ieh.uni-stuttgart.de; stefan.tenbohlen@ieh.uni-stuttgart.de).

K. A. Alsdorf is with TransnetBW GmbH, Wendlingen, 73240 Germany (email: k.alsdorf@transnetbw.de).

Paper submitted to the International Conference on Power Systems Transients (IPST2023) in Thessaloniki, Greece, June 12-15, 2023.

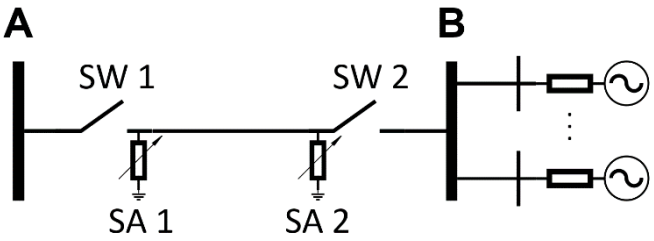

Fig. 1. Schematic diagram of the circuit implemented in ATP to simulate the energization of transmission line A-B.

The geometry and electrical parameters of the overhead lines were used to calculate the transmission line parameters, including the bundle configuration. However, the tower dimensions were estimated. Besides the connection to Substation A, Substation B has five other connections. The corresponding transmission lines were modeled using the same method applied to line A-B. A source of 420 kV and an inductance of 100 mH are connected to each of the other five substations and represent the respective equivalent circuit. Finally, the surge arresters were modeled as nonlinear resistances, considering a typical voltage-current curve for a 360 kV class IV surge arrester. There is only one surge arrester, installed in phase A, on each side of the transmission line A-B. Fig. 2 shows the simulated transient voltages in substation A when the switch SW 2 (substation B) is closed at 3.5 ms. The same signals are used later for comparison with the measured values.

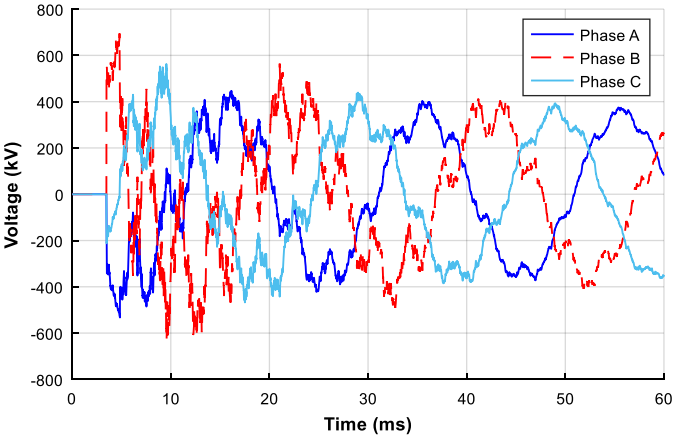

Fig. 2. Simulated transient voltage in substation A at SA 1 during the closing operation of the transmission line A-B in substation B.

In this simulation, the highest overvoltage occurs in phase B with a peak value of 695 kV, whereas phase C has a maximum overvoltage of 563 kV and phase A 447 kV, but this is limited by the surge arrester. The calculated energy through the surge arrester SA 1 during the transient was about 11 % of its energy capability and was, therefore, insufficient to cause the failure.

The maximum voltage value depends on the switching time. Then, further simulations were carried out using statistical switches with Gaussian distribution to determine the maximum overvoltage considering different switching times [18]. The maximum calculated overvoltage was 794 kV.

III. The Measurement System

The transient overvoltage during the energization of transmission line A-B when the surge arrester SA 1 failed was not recorded. In addition, the CVT presents a distorted output voltage during fast transients. Therefore, an automated measurement system has been developed to record transient voltages in a substation environment for long-term evaluation.

A. Concept

The measurement device is based on the principle of a capacitive electric field sensor, and its output is connected to a broadband power quality monitor (PQM) to record the transients. The schematic diagram of the measurement system is presented in Fig. 3.

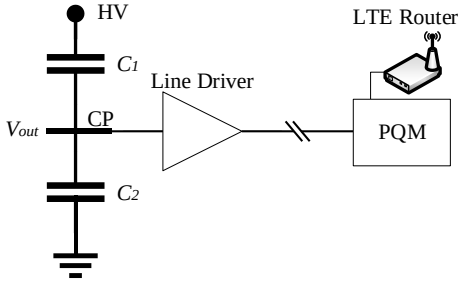

Fig. 3. Schematic diagram of the measurement system for transient voltages.

The capacitance C_1 is given by the stray capacitance between the high voltage connection (HV) and the coupling plane (CP), whereas the capacitance C_2 is user-defined depending on the calculated voltage ratio. The measurement device works as a capacitive voltage divider, and the output voltage V_{out} can be calculated according to (1).

$$V_{out} = V_{HV} \frac{C_1}{C_1 + C_2} \quad (1)$$

where V_{HV} is the input voltage measured between HV and ground.

A coaxial cable (approximately 15 m) connects the output of the capacitive divider setup to a PQM. For this reason, the device has an analog line driver, so the cable impedance does not affect the voltage ratio. The PQM records both, steady-state RMS values of the output voltage and transient signals. Finally, transients are uploaded to a remote server via LTE router (and the measurements can be visualized and evaluated in a web terminal) for detailed evaluation.

B. Estimation of the Stray Capacitance

To define the capacitance C_2 and calculate the required voltage ratio given by the PQM input range, the stray capacitance C_1 (where the system will be installed) must be estimated. In this case study, the capacitive divider setup is installed on the base of a disconnector, and consequently, the stray capacitance depends on the distance between its base (grounded) and the contact rod. Therefore, the stray capacitance was calculated by modeling the disconnector with real dimensions in the electromagnetic field simulation software CST Studio Suite® [19] using the electrostatic solver. The model is shown in Fig. 4.

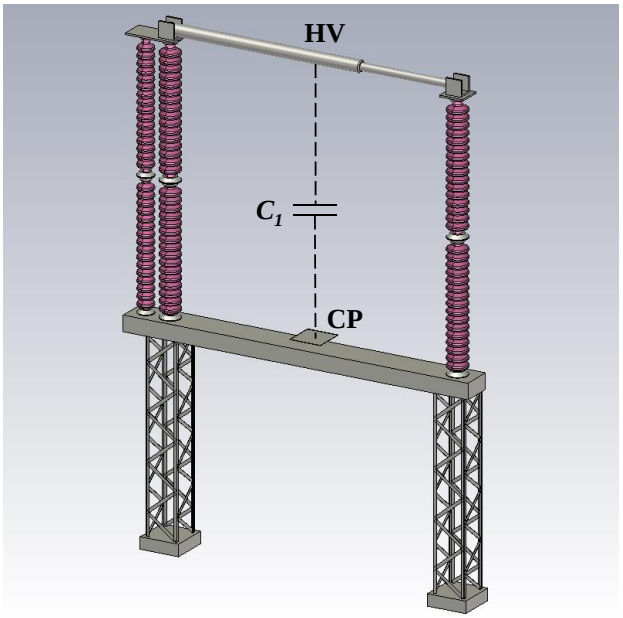

Fig. 4. Modeling of the air insulated disconnector for calculation of C_1.

The calculated value of the stray capacitance C_1 is 0.86 pF. Then, considering a maximum input voltage V_{HV} = 1 MV_{peak} and a maximum output voltage V_{out} = 20 V_{peak}, the capacitance C_2 is calculated as 43 nF. Furthermore, the coupling plane has a stray capacitance of 37.9 pF to the grounded base of the disconnector. However, it has practically no influence on the voltage ratio because it is in parallel with C_2, which is much higher.

C. Hardware Design

The measurement system consists of two essential elements: the capacitive divider setup and the control cabinet, where the transients are stored and transmitted to a server.

1) Capacitive Divider Setup

The development of the capacitive divider setup started with the selection of the material and size of the coupling plane. A 40 cm x 40 cm aluminum plate is used in this case. Then an electronic circuit board was designed, containing the capacitance C_2 and the line driver. C_2 can be set between 8.3 nF and 49.8 nF by connecting up to 6 temperature-stable capacitors of 8.3 nF in parallel. The circuit board is supplied by a 24 V_{DC} source. Fig. 5. shows the coupling plane and the box with the electronic circuit.

2) Control Cabinet

The output signal from the capacitive divider setup is sent via coaxial cable to a power quality monitor located in a control cabinet. The installed PQM is the PQM-800, which has a sample rate of 1 MS/s, 8 input channels, and an internal storage of 512 GB. The recording length of transient signals is adaptive from 3 to 10 cycles (of power frequency), depending on the number of cycles affected [20]. The PQM measures signals up to 500 kHz. Therefore, the frequency range of the measurement system is 50 Hz to 500 kHz.

Besides the PQM, the cabinet has a 24 V_{DC} source to supply the line drivers, and an LTE router to transmit the transients to a server. Fig. 6 shows the control cabinet with the components.

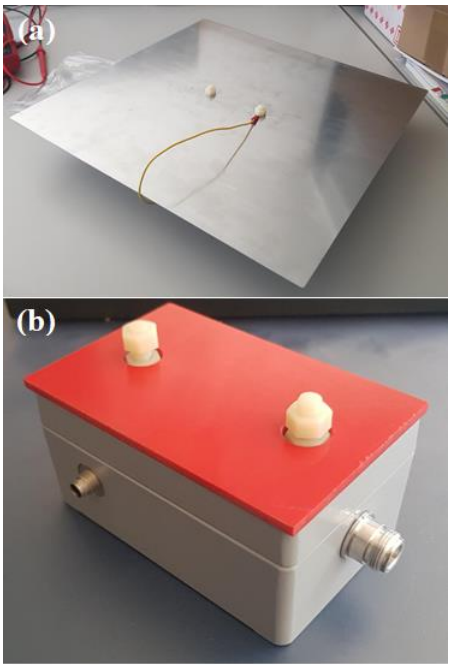

Fig. 5. The capacitive divider setup. (a) Coupling plane. (b) Box with the electronic circuit board (C_2, overvoltage protection, and line driver).

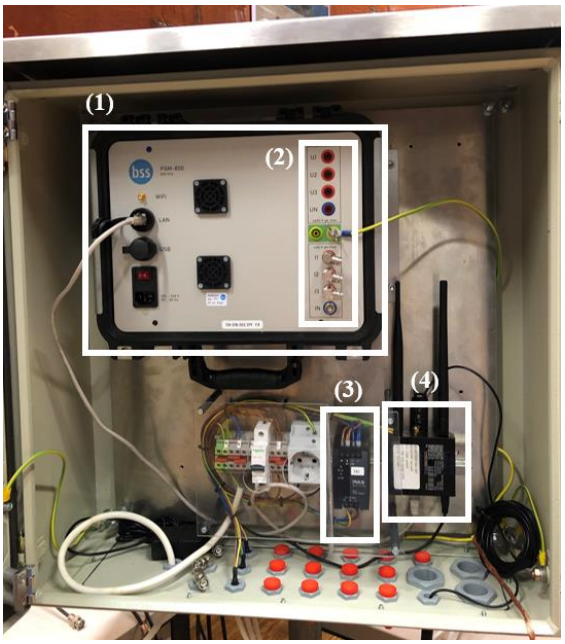

Fig. 6. The control cabinet. (1) PQM-800. (2) Input channels. (3) 24 V_{DC} source. (4) LTE router.

IV. System Evaluation in the High Voltage Laboratory

After designing and assembling the three capacitive divider setups, they were tested in the high-voltage laboratory of the Institute of Power Transmission and High Voltage Technology at the University of Stuttgart. First, the linearity of the output voltage was evaluated as a function of the input voltage by measuring the voltage ratio at 50 Hz. Since the device operates as a capacitive divider, linear behavior is expected. Fig. 7 shows the schematic diagram and the setup in the laboratory to measure the voltage ratio.

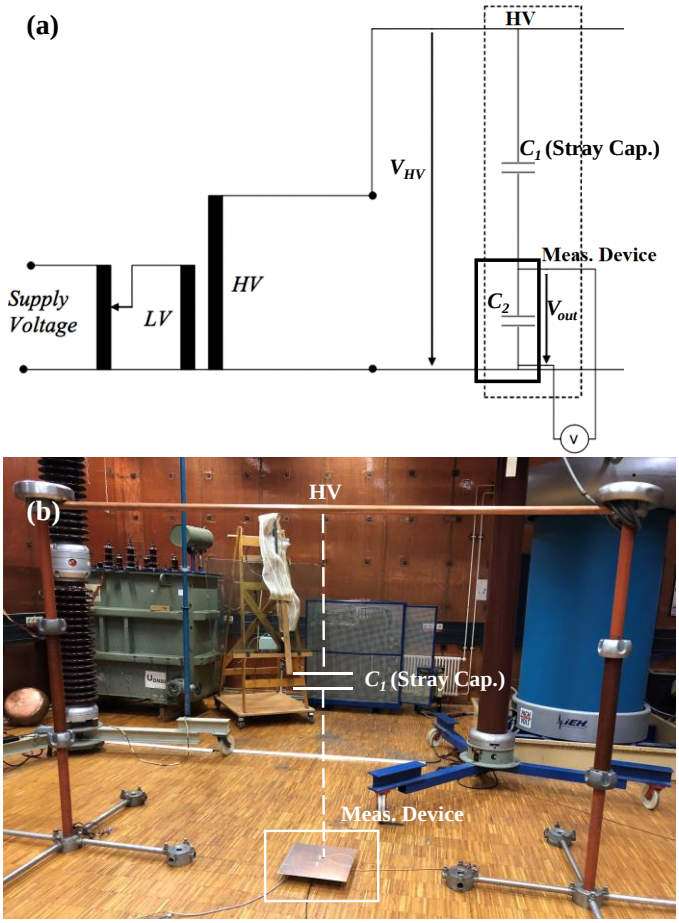

Fig. 7. Measurement of the voltage ratio. (a) Schematic diagram. (b) Test setup in the high voltage laboratory.

For example, the measurement of the voltage ratio of one device was done with an input voltage from 7.84 kV_{rms} to 128.40 kV_{rms}, and the results were adequate, with a mean value of 109891:1 and a maximum variation of 0.98 %. It is important to note that the voltage ratio depends directly on the stray capacitance C_1 and, consequently, on the distance between HV and the coupling plane. Thus, the device has a different voltage ratio when installed in the substation, and calibration is therefore necessary. A lightning impulse test was also done in the high-voltage laboratory for both full and chopped waves. In the tests with chopped wave, the fall time from 90 % of the peak value to 0 was measured for all devices. The results were satisfactory.

V. Installation in the Substation

The measurement system was installed in substation A after completion of the tests. The three capacitive divider setups were installed on the disconnector bases of the line A-B. Then, they were connected to the substation grounding system and two cables (for each device) were installed between the devices and the control cabinet, one for the 24 V_{DC} supply and the other for the output signal. The control cabinet was installed at the concrete base of the circuit breaker of the same bay, approximately 6 m from the disconnectors. Fig. 8 shows one of the capacitive divider setups installed on the base of the disconnector.

Fig. 8. Installation of the capacitive divider setups. (a) Overview of the installation. (b) Detail of one installed capacitive coupling plane.

A. Calibration of the Voltage Ratio

As mentioned in Section IV, the voltage ratio depends on the physical configuration where the capacitive divider setups are installed, since the stray capacitance C_1 changes with the distance between HV and the coupling plane of the device. Moreover, the adjacent phases also influence the ratio of the device, because there is a stray capacitance between the HV of these phases and the coupling plane of the device. For example, the device installed in phase B is affected by the stray capacitance of phase B itself, the stray capacitance between phase A and the coupling plane, and the stray capacitance between phase C and the coupling plane. For this reason, a lower output voltage is expected for phase B, which means a higher voltage ratio. Ideally, the devices installed in phases A and C should have the same output voltage and voltage ratio because they are equally influenced by phase B.

In this case study, there is another important point to consider. There is another bay on each side of the bay of line A-B, which also influence the output voltage of the capacitive divider setups, because of the undesired coupling. The most significant influences were observed in phase A, which is influenced by phase C of one adjacent bay, and phase C, influenced by phase A of the other adjacent bay. This could be checked when the transmission line was out of service and the measurement system was still measuring a signal of about 23 kV for phase C, for example. For a better understanding, this configuration is shown in Fig. 9.

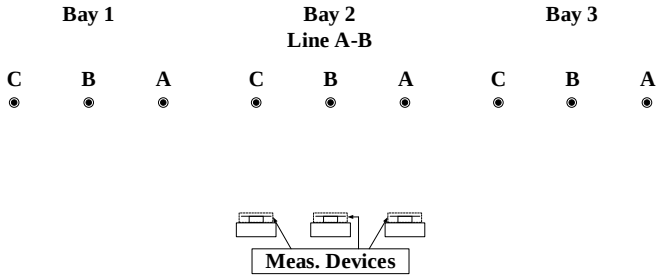

Fig. 9. Configuration of the bay of line A-B with two adjacent bays.

The three devices were calibrated using the steady-state voltage measured by a capacitive voltage transformer as a reference. The calibration was done directly in the PQM, where the voltage ratio can be set independently for each input channel. Because of the different influences of adjacent phases, each device was calibrated with a different voltage ratio, in this case, 117460.9:1, 141931.9:1, and 126161.7:1 for phases A, B, and C, respectively.

VI. Measurement Results

The last step of this study is the evaluation of the transients measured in the substation and recorded by the PQM. During a measurement campaign of three months, many voltage transients were recorded. Since this work focuses on analyzing the overvoltage caused by the energization of a transmission line, only these transients are presented. Fig. 10 shows the comparison between the measured and simulated signals for a closing operation at 3.5 ms. These signals represent the voltages of transmission line A-B in substation A at SA 1.

The maximum measured voltages are 429 kV, 775 kV, and 446 kV for phases A, B, and C, respectively. For the simulated results, the maximum voltages are 447 kV, 695 kV, and 563 kV, respectively. The maximum measured voltage of 775 kV is 2.4 % lower than the maximum value of 794 kV obtained in the simulations and presented in Section II.

In general, the measured and simulated signals have good correspondence, although the simulated signals show more oscillations in the first periods. These effects may be related to the fact that not all transmission line parameters are known and some of them are estimated.

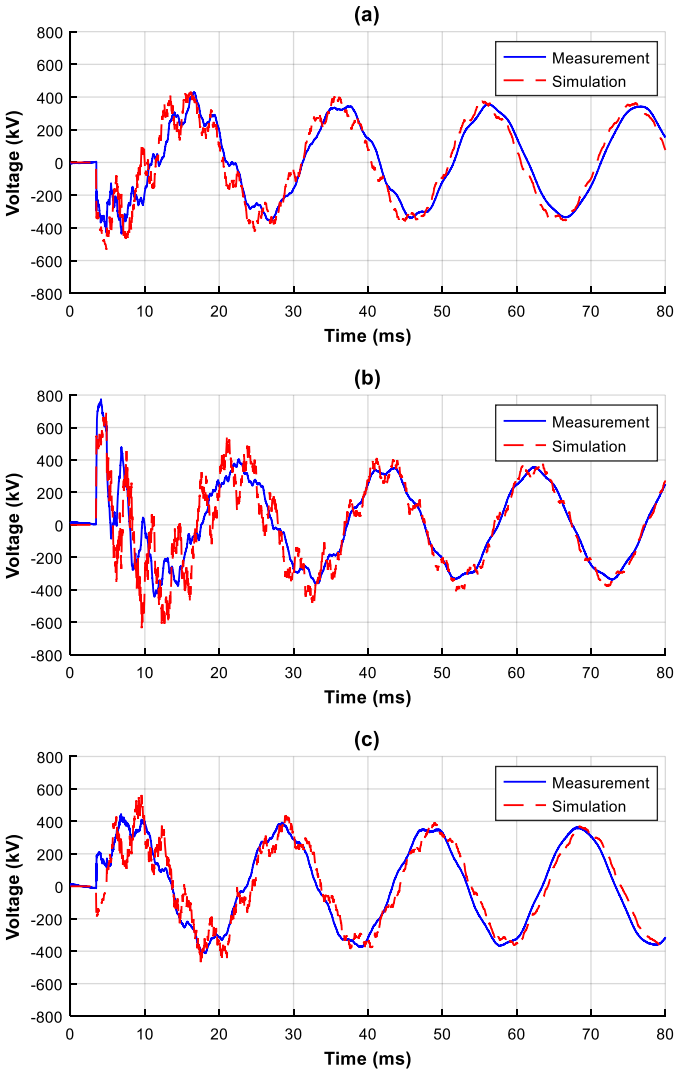

Fig. 10. Measured and simulated transient overvoltages during a closing operation of the line A-B. (a) Phase A. (b) Phase B. (c) Phase C.

VII. Discussions

A. Simulation of Electromagnetic Transients

Transmission line modeling is a complex and specific topic where the chosen method and parameters play an important role. In this case study, simulating the energization of a transmission line in an electromagnetic transient simulation program was only one step to investigate the failure of a surge arrester. The objective of this simulation was to approximately predict the transient overvoltage. Therefore, the use of some estimated parameters did not have a negative impact on the results obtained.

B. Influence of Adjacent Bays

The adjacent bays influenced the output voltage of the capacitive divider setups installed in the substation due to undesired coupling. Therefore, this is a relevant point to consider when using this system. For example, if one of the adjacent bays is out of service, the voltage ratio will deviate from the pre-calibrated value, and the capacitive divider setups will present a larger error. Thus, the status of the adjacent bays should be considered when analyzing the measured transients.

VIII. Conclusions

A reliable measurement system must be used to accurately measure fast transients such as lightning or switching. Voltage transformers are normally used for voltage measurement in high-voltage substations, but they do not have a linear response for high-frequency signals. In this paper, we presented a broadband measurement system based on a capacitive electric field sensor, which has been demonstrated to be capable of measuring switching transient voltages of a 420 kV transmission line.

The starting point for this study was the failure of a surge arrester during the energization of a transmission line. For this reason, this work focused on the closing operation, but the developed system can be applied to other measurements of transient voltages. Many different transient signals were recorded during the measurement campaign and can therefore be the focus of further studies.

The measurement and simulation results have a good correlation. Therefore, the conclusion is that the transient overvoltages caused by the energization of the transmission line should not lead to the failure of the surge arrester. Further investigation is needed to determine the cause of failure, considering other factors such as loss of tightness, moisture ingress, aging, and mishandling during storage or transport.

Finally, it is important to mention that installing the developed measurement system onsite is relatively simple and does not require de-energizing the bay where it will be installed. Therefore, it can be considered a flexible solution for the long-term monitoring of transient overvoltages in substations.

IX. References

[1] A. V. Dedinho, A. B. F. D. Schneider, A. N. de Souza and P. da Costa Junior, "Electromagnetic transients in transmission lines using the Modelica modeling language and identification of failures in underground cables for power quality improvement," (in Portuguese), in *XIX Congresso Brasileiro de Automática*, Campina Grande, PB, Brazil, 2012, pp. 4860-4866.

[2] IEC 60071-1, "Insulation co-ordination - Part 1: Definitions, principles and rules", Ed. 9.0, 2019.

[3] IEC 60071-2, "Insulation co-ordination - Part 2: Application guidelines", Ed. 4.0, 2018.

[4] IEC 60071-4, "Insulation co-ordination - Part 4: Computational guide to insulation co-ordination and modelling of electrical networks", Ed. 1.0, 2004.

[5] CIGRE TB 577A, "Electrical transient interaction between transformers and the power system - Part 1: Expertise", JWG A2/C4.39, 2014.

[6] CIGRE TB 577B, "Electrical transient interaction between transformers and the power system - Part 2: Case studies", JWG A2/C4.39, 2014.

[7] CIGRE TB 881, "Electromagnetic transient simulation models for large-scale system impact studies in power systems having a high penetration of inverter-connected generation", WG C4.56, 2022.

[8] F. L. Probst, "Modeling of a Capacitive Voltage Transformer for Evaluation of Transient Behavior," (in Portuguese), M.S. Thesis, Depto. Elect. Eng., Fed. Univ. of Santa Catarina, Florianopolis, SC, Brazil, 2020.

[9] H. J. Vermeulen and P. Davel, "Voltage harmonic distortion measurements using capacitive voltage transformers," Proceedings of IEEE. AFRICON '96, 1996, pp. 1012-1017 vol.2, doi: 10.1109/AFRCON.1996.563035.

[10] M. H. Zare, A. Mirzaei and H. Askarian Abyaneh, "Designing a compensating electronic circuit to enhance capacitive voltage transformer characteristics," The 9th Power Systems Protection and Control Conference (PSPC2015), 2015, pp. 12-18, doi: 10.1109/PSPC.2015.7094922.

[11] L. Tong, Y. Liu, Y. Chen, S. Su and P. Liang, "A CVT Based Lightning Impulse Wave Measuring Method Using Convolutional Neural Network," 2021 IEEE 4th International Electrical and Energy Conference (CIEEC), 2021, pp. 1-6, doi: 10.1109/CIEEC50170.2021.9511055.

[12] H. K. Zadeh and L. Zuyi, "A compensation scheme for CVT transient effects using artificial neural network," Electric Power Systems Research 78, no. 1, 2008, pp. 30-38, doi: 10.1016/j.epsr.2006.12.006.

[13] Y.c. Kang, T.Y. Zheng, S.W. Choi, Y.H. Kim, Y.G. Kim, S.1. .lang, S.H. Kang, Design and Evaluation of a Compensating Algorithm for the Secondary Voltage of a Coupling Capacitor Voltage Transformer in the Time Domain, lET Gener. Transm. Distrib., vol. 3 n. 9, 2008, pp. 793-800, doi: 10.1049/iet-gtd.2008.0563.

[14] T. Stirl: "Online-Monitoring von kapazitiv gesteuerten Durchführungen an Leistungstransformatoren", ETG technical seminar, Cologne, 2004.

[15] T. Stirl, R. Skrzypek, S. Tenbohlen and R. Vilaithong, "On-line Condition Monitoring and Diagnosis for Power Transformers their Bushings, Tap Changer and Insulation system," 2006 International Conference on Condition Monitoring and Diagnosis (CMD), Changwon, Korea, 2006.

[16] G. -M. Ma, C. -R. Li, J. -T. Quan and J. Jiang, "Measurement of VFTO Based on the Transformer Bushing Sensor," in IEEE Transactions on Power Delivery, vol. 26, no. 2, pp. 684-692, April 2011, doi: 10.1109/TPWRD.2010.2042467.

[17] M. Khatir, S. A. Zidi, M. K. Fellah, S. Hadjeri and O. Dahou, "HVDC Transmission Line Models for Steady-State and Transients Analysis in SIMULINK Environment," IECON 2006 - 32nd Annual Conference on IEEE Industrial Electronics, 2006, pp. 436-441, doi: 10.1109/IECON.2006.347234.

[18] J. A. Martinez, R. Natarajan and E. Camm, "Comparison of statistical switching results using Gaussian, uniform and systematic switching approaches," 2000 Power Engineering Society Summer Meeting (Cat. No.00CH37134), Seattle, WA, USA, 2000, pp. 884-889 vol. 2, doi: 10.1109/PESS.2000.867477.

[19] CST Studio Suite [Computer software], 2021. Available: http://www.cst.com.

[20] BSS Hochspannungstechnik, "PQM-800 Power Quality Monitor", PQM-800 datasheet [Online], v. 2.0. Available: https://bss-hochspannungstechnik.de/pdf/Datasheet%20PQM-800.pdf.